

# Saving fuel using wireless vehicle-to-vehicle communication

Chaozhe R. He and Gábor Orosz

**Abstract**—In this paper, we compare two different connected cruise control strategies that utilize vehicle-to-vehicle (V2V) communication to monitor multiple vehicles ahead in order to save fuel. One strategy uses direct feedback while the other is based on dynamic optimization that assigns the control action in a receding horizon fashion while relying on preview information about the vehicle immediately ahead. We demonstrate that both methods produce significant fuel improvements but the performance of the second controller depends significantly on the length of time horizon as well as the accuracy of the preview information.

## I. INTRODUCTION

Heavy-duty vehicles (HDVs) account for a significant share of fuel consumption in the transportation sector [1], [2]. The wide use of sensors and information networks enables previewing geological information (road elevation, wind speed) and can lead to significant fuel savings for HDVs under sparse traffic [3], [4]. The problem can become much more challenging in dense traffic conditions, due to the difficulties in getting reliable information about the surrounding traffic [5].

Wireless vehicle-to-vehicle (V2V) communication may be used to acquire information beyond line of sight. By appropriately fusing sensory and V2V information, one may reduce traffic congestion and improve the overall fuel efficiency of the traffic flow [6], [7]. In particular, one may apply the concept of connected cruise control (CCC) that utilizes motion information from multiple vehicles ahead [8]. The simplest way of implementing CCC is to use the available information directly with constant gains and optimize these gains in order to achieve the best possible fuel economy with a fixed controller structure [9]. The advantage of this approach is that the optimization can be carried out offline and that the implementation of the controller is straightforward and can be tuned to drive similar to human drivers.

Another CCC strategy is utilize V2V information to predict the future speed/position of the vehicle immediately ahead for a given time horizon [10] and then apply rolling horizon optimal control (RHOC) (often called model predictive control (MPC)) [11], [12]. Potentially dynamic optimization may lead to better fuel economy than the static one but the lack of predefined control structure may lead to motion that is very different from that of the human drivers. Moreover, RHOC relies on preview information about the motion of the vehicle ahead of preceding vehicle over a long

time horizon (more than 10s) [13], while a reliable prediction is typically only available for few seconds [14]. To bypass such uncertainty in prediction, some researchers model the speed of preceding vehicle as stochastic process and optimize fuel using stochastic dynamic programming [15].

In this paper, we compare the two different CCC strategies explained above in terms of fuel economy improvements. In particular, we optimize the feedback gains for the feedback-based CCC and vary the length of the preview horizon as well as the accuracy of the preview information for the RHOC-based CCC. Numerical simulations are used to compare to different approaches and trade-offs have been identified.

## II. MODELING

In this section, we describe the models used in this paper, including vehicle dynamics, fuel consumption map and input/state constraints.

### A. Vehicle Dynamics

The longitudinal dynamics of the HDV is derived using classical mechanics. We assume that no slip occurs at the wheels and that the flexibility of the tires and the suspension can be neglected. Then using the power law we obtain

$$m_{\text{eff}}\dot{v} = mg \sin \phi + \gamma mg \cos \phi + \kappa_0(v + v_w)^2 + \frac{\eta T_e + T_b}{R}, \quad (1)$$

see [4], where the effective mass  $m_{\text{eff}} = m + I/R^2$  contains the mass of the vehicle  $m$ , the moment of inertia  $I$  of the rotating elements, and the wheel radius  $R$ . Furthermore,  $g$  is the gravitational constant,  $\phi$  is the inclination angle,  $\gamma$  is the rolling resistance coefficient,  $\kappa_0$  is the air drag constant,  $v_w$  is the speed of the headwind,  $\eta$  is the gear ratio (that includes the final drive ratio and the transmission efficiency). Moreover, the engine torque  $T_e$  is assumed to be non-negative while the braking torque  $T_b$  applied on the axle is assumed to be non-positive. See [4] for parameter values used in this paper that are for a Prostar truck manufactured by Navistar. Based on (1), we have

$$\dot{v} = -a \sin \phi - b \cos \phi - \kappa(v + v_w)^2 + u, \quad (2)$$

where

$$a = \frac{mg}{m_{\text{eff}}}, \quad b = \frac{\gamma mg}{m_{\text{eff}}}, \quad \kappa = \frac{\kappa_0}{m_{\text{eff}}}, \quad u = \frac{\eta T_e + T_b}{m_{\text{eff}} R}. \quad (3)$$

Throughout the paper, we consider the vehicle traveling on flat road with no headwind, i.e.,  $\phi \equiv 0$  and  $v_w = 0$ . Thus, (2) simplifies to

$$\dot{v} = \underbrace{-b - \kappa v^2}_{:=f(v)} + u. \quad (4)$$

This work was supported by the University of Michigan Mobility Transformation Center

Chaozhe R. He and Gábor Orosz are with the Department of Mechanical Engineering, University of Michigan, Ann Arbor, Michigan, 48109, U.S.A. {hchaozhe, orosz}@umich.edu

We remark that this setup enables us to decouple the optimization of the gear change map and the speed profile. In particular, we assume that the gear change map is given and we focus our attention on minimizing the fuel consumption by designing  $u$ .

### B. Fuel consumption map and input constraints

Fuel consumption rates are typically given as a function of the engine speed  $\omega_e$  and engine torque  $T_e$ , that is,  $q(\omega_e, T_e)$ . Given a control input  $u$  at a certain speed  $v$ , different gears set the engine to different working points. For a well-designed gear shift logic one can assign a unique gear for each  $v$  and  $u$ , such that the transformation

$$(u, v) = \left( \frac{R\omega_e}{\eta}, \frac{\eta T_e}{m_{\text{eff}} R} \right) \quad (5)$$

is well-defined [16]. This way the fuel consumption map  $q(\omega_e, T_e)$  is transformed to  $q(v, u)$ . One may fit Willans approximation

$$q(v, u) = \begin{cases} p_2 v u + p_1 v + p_0, & \text{if } u \geq 0, \\ p_1 v + p_0, & \text{if } u < 0, \end{cases} \quad (6)$$

to data in order to get an analytical approximation of the fuel consumption rate [17]. The distinction between the two cases is made since for  $u < 0$  then engine torque is set to zero as the vehicle applies braking. In particular for the Maxxforce engine used in the Prostar truck we obtain  $p_2 = 1.8284 \pm 0.0019$  [gs<sup>2</sup>/m<sup>2</sup>],  $p_1 = 0.0209 \pm 0.0006$  [g/m],  $p_0 = -0.1868 \pm 0.0068$  [g/s]; see [4], [16].

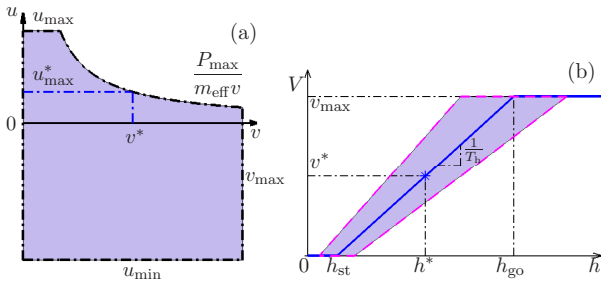


Fig. 1: (a) The working region (7,8) is indicated by blue shading in the  $(v, u)$ -plane. (b) The range policy function (12) shown by the blue solid curve. The blue shaded area corresponds to the constraints in (17).

Due to the power limitations of the engine and the torque limitations of the brakes we also obtain constraints on the rescaled torque  $u$ . The upper bound consists of two segments, a constant section at  $u_{\text{max}}$  for low speed and an iso-power curve at  $P_{\text{max}}$  for higher speed, while the lower bound is given by the constant  $u_{\text{min}}$ . Since  $P = T_e \omega_e = m_{\text{eff}} u v$ , we have

$$u_{\text{min}} \leq u \leq \min \left\{ u_{\text{max}}, \frac{P_{\text{max}}}{m_{\text{eff}} v} \right\}. \quad (7)$$

In this paper we use  $u_{\text{max}} = 2$  [m/s<sup>2</sup>],  $P_{\text{max}} = 300.65$  [kW], and  $u_{\text{min}} = -3$  [m/s<sup>2</sup>] that are acquired through data fitting.

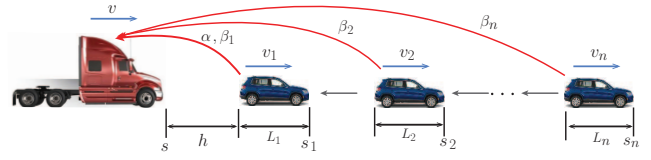


Fig. 2: Layout of the connected vehicle system with a HDV vehicle at the tail controlled by a CCC algorithm. Each preceding vehicle is reacting to motion of the vehicle immediately ahead while the truck utilizes V2V information about  $n$  vehicles ahead.

The constraints (7) together with the speed constraints

$$0 \leq v \leq v_{\text{max}}, \quad (8)$$

are indicated by the blue shaded domain in Fig. 1(a).

### III. CAR-FOLLOWING PROBLEM SETUP

In this section, we first describe the traffic flow using car following models. We then formulate the two different CCC strategies that exploit V2V information to improve the fuel economy.

#### A. Car-following models

Assume that the CCC vehicle could utilize V2V information from  $n$  vehicles ahead (see Fig. 2) and that these preceding vehicles are controlled by human drivers who react only to the motion of the vehicle immediately ahead. Thus, the longitudinal dynamics of the preceding vehicles are given by

$$\begin{aligned} \dot{s}_i &= v_i, \\ \dot{v}_i &= u_i(s_i, s_{i-1}, v_i, v_{i-1}; p_i), \end{aligned} \quad (9)$$

for  $i = 1, \dots, n-1$ , where dot denotes differentiation with respect to time  $t$ , the symbols  $s_i$  and  $v_i$  denote the position and the speed of the  $i$ -th vehicle, and  $p_i$  corresponds to the parameters used in the control strategy  $u_i$ .

In particular, we assume that the preceding vehicles use the car-following rule

$$u_i = \alpha_{h,i} (V(s_{i+1} - s_i - L_{i+1}) - v_i) + \beta_{h,i} (v_{i+1} - v_i), \quad (10)$$

to control their longitudinal motion. Here  $\alpha_{h,i}$  and  $\beta_{h,i}$  denote the control gains while the human reaction time is neglected for simplicity. Moreover,  $L_{i+1}$  denotes the length of the  $i+1$ -th vehicle and range policy  $V(h)$  gives the desired speed of the driver as a function of the headway

$$h_i = s_{i+1} - s_i - L_{i+1}, \quad (11)$$

see Fig. 2. For small headway  $h \leq h_{\text{st}}$  the vehicle is expected to stop; for large headway  $h \geq h_{\text{go}}$  it is expected to travel with the maximum speed  $v_{\text{max}}$ ; between  $h_{\text{st}}$  and  $h_{\text{go}}$  the desired speed shall increase monotonically with the headway [8].

In this paper, we use the range policy

$$V(h) = \begin{cases} 0 & \text{if } h \leq h_{\text{st}}, \\ v_{\text{max}} \frac{h - h_{\text{st}}}{h_{\text{go}} - h_{\text{st}}} & \text{if } h_{\text{st}} < h < h_{\text{go}}, \\ v_{\text{max}} & \text{if } h \geq h_{\text{go}}, \end{cases} \quad (12)$$

that is shown in Fig. 1(b) as a blue solid curve. Between  $h_{st}$  and  $h_{go}$  this corresponds the constant time headway

$$T_h = \frac{h_{go} - h_{st}}{v_{max}}. \quad (13)$$

Here we set  $h_{st} = 5[\text{m}]$ ,  $h_{go} = 35[\text{m}]$ , and  $v_{max} = 30[\text{m/s}]$  that yields  $T_h = 1[\text{s}]$  corresponding to an average driver. We remark that smaller  $h_{st}$  and smaller  $T_h$  typically correspond to more aggressive drivers while larger  $h_{st}$  and larger  $T_h$  typically correspond to more cautious drivers. The magenta curves enclosing the blue shaded domain indicate some of these scenarios when compared to the blue curve.

Finally, note that (9,10,11) admit a so-called uniform flow equilibrium

$$h_i(t) \equiv h^*, \quad v_i(t) \equiv v^* = V(h^*), \quad (14)$$

where equidistant vehicles follow each other with the same speed. This is indicated in Fig. 1(b) as a blue star. In this paper we will investigate the dynamics in the vicinity of the equilibrium with  $h^* = 20[\text{m}]$  and  $v^* = 15[\text{m/s}]$ .

### B. Feedback-based CCC

In this framework we use the received V2V information explicitly in order to design the dynamics of the CCC vehicle. In particular, to mimic the behaviour of human drivers described by (9,10) while still exploiting the velocity information obtained via V2V communication from  $n$  vehicles ahead, we consider the control law

$$u = -f(v) + \alpha \left( V(s_1 - s - L_1) - v \right) + \sum_{j=1}^n \beta_j (v_j - v). \quad (15)$$

where  $V$  denotes the range policy function defined in (12). Substituting this into (4) we obtain

$$\begin{aligned} \dot{s} &= v, \\ \dot{v} &= \alpha \left( V(s_1 - s - L_1) - v \right) + \sum_{j=1}^n \beta_j (v_j - v). \end{aligned} \quad (16)$$

Notice that including the dissipative term  $f(v)$  in the control law (15) allows us to cancel this term. This may also be achieved by other methods, e.g., by using integral action [8]. Also notice that (16) also satisfies the equilibrium (14) (without index  $i$ ).

In order to minimize the fuel economy we optimize the control gains  $\alpha$  and  $\beta_j$ ,  $j = 1, \dots, n$  similar to [9]. When running numerical simulations the constraints (7,8) will also be enforced.

### C. RHOC-based CCC

In this framework we use the received V2V information implicitly. Assuming that preview information about the position of the vehicle immediately ahead can be constructed over the time horizon  $T$  using the received V2V information, we apply receding horizon optimal control along the sample

period  $\Delta T$ . That is, the following optimal control problem is solved at each  $t_j = j\Delta T$

$$\begin{aligned} &\text{Minimize} && \int_{t_j}^{t_j + T} q(u, v) dt, \\ &\text{Subject to} && \begin{bmatrix} \dot{s} \\ \dot{v} \end{bmatrix} = \begin{bmatrix} v \\ f(v) + u \end{bmatrix}, \\ &&& v \bar{T}_h + \bar{h}_{st} \leq s_1 - s - L_1 \leq v \bar{T}_h + \bar{h}_{st}, \\ &&& \begin{bmatrix} s(t_j) \\ v(t_j) \end{bmatrix} = \begin{bmatrix} s(j\Delta T) \\ v(j\Delta T) \end{bmatrix}, \end{aligned} \quad (17)$$

and the constraints (7,8) shall also be satisfied. The time horizon and the sample time is chosen such that  $T = N\Delta T$  for some  $N \in \mathbb{N}$ . In order to generate trajectories that stay close to the range policy (12) we included some state constraints in (17). These together with (8) are shown by the blue shaded region in Fig. 1(b).

RHOC algorithms are typically designed and implemented in discrete-time in coordination with the sample period  $\Delta T$ . However, such discretization may lead to ‘‘jerky’’ trajectories. To avoid such phenomena we define the control inputs  $u_d$  and  $u_b$  such that

$$u = u_d + u_b, \quad u_b u_d = 0. \quad (18)$$

In fact,  $u_d = \frac{\eta T_c}{m_{\text{eff}} R}$  is the rescaled driving torque, while  $u_b = \frac{T_b}{m_{\text{eff}} R}$  is the rescaled braking torque; cf. (2,3). Then we pose the following constraints

$$\dot{u}_d < \Delta \bar{u}, \quad \dot{u}_b > \Delta \underline{u}. \quad (19)$$

On the other hand, to simplify the optimal control problem (7,8,17) the following linear approximations are made. First, we construct linear approximation of  $f$  (cf. (4)) around the equilibrium value  $v^*$ , that is,

$$\hat{f}(v) = -b - \kappa v^* v. \quad (20)$$

Second, (7) is substituted by the simplified version

$$u_{\min} \leq u \leq u_{\max}^*, \quad (21)$$

where  $u_{\max}^* = \min \left\{ u_{\max}, \frac{P_{\max}}{m_{\text{eff}} v^*} \right\}$  is constant in the whole speed domain (8); see Fig. 1.

Thus, (8,17,19,21) are discretized using explicit Euler method with time step  $\Delta T$  yielding

Minimize

$$\sum_{k=0}^{N-1} \left( \frac{1}{2} \begin{bmatrix} \mathbf{x}(k|t_j) \\ \mathbf{u}(k|t_j) \end{bmatrix}^T \mathbf{Q} \begin{bmatrix} \mathbf{x}(k|t_j) \\ \mathbf{u}(k|t_j) \end{bmatrix} + \mathbf{P} \mathbf{x}(k|t_j) \right) \Delta T,$$

Subject to  $\mathbf{x}(k+1|t_j) = \mathbf{A} \mathbf{x}(k|t_j) + \mathbf{B} \mathbf{u}(k|t_j) + \mathbf{d}$ ,

$$\mathbf{W} \mathbf{x}(k|t_j) \leq \mathbf{g}(k|t_j),$$

$$\mathbf{x}(0|t_j) = \mathbf{x}(t_j),$$

$$\underline{\mathbf{u}} \leq \mathbf{u}(k|t_j) \leq \bar{\mathbf{u}},$$

$$u_d(k+1|t_j) - u_d(k|t_j) \leq \Delta \bar{u} \Delta T,$$

$$u_b(k|t_j) - u_b(k+1|t_j) \leq -\Delta \underline{u} \Delta T, \quad (22)$$

where

$$\begin{aligned} \mathbf{x} &= \begin{bmatrix} s \\ v \end{bmatrix}, \quad \mathbf{u} = \begin{bmatrix} u_d \\ u_b \end{bmatrix}, \\ \mathbf{Q} &= \begin{bmatrix} 0 & 0 & 0 & 0 \\ 0 & 0 & p_2 & 0 \\ 0 & p_2 & 0 & 0 \\ 0 & 0 & 0 & 0 \end{bmatrix}, \quad \mathbf{P} = \begin{bmatrix} 0 \\ p_1 \\ 0 \\ 0 \end{bmatrix}, \\ \mathbf{A} &= \begin{bmatrix} 1 & \Delta T \\ 0 & 1 - \kappa v^* \Delta T \end{bmatrix}, \quad \mathbf{B} = \begin{bmatrix} 0 & 0 \\ \Delta T & \Delta T \end{bmatrix}, \\ \mathbf{d} &= \begin{bmatrix} 0 \\ -b \Delta T \end{bmatrix}, \quad \underline{\mathbf{u}} = \begin{bmatrix} 0 \\ u_{\min} \end{bmatrix}, \quad \bar{\mathbf{u}} = \begin{bmatrix} u_{\max}^* \\ 0 \end{bmatrix}, \\ \mathbf{W} &= \begin{bmatrix} -1 & -\bar{T}_h \\ 1 & \underline{T}_h \\ 0 & -1 \\ 0 & 1 \end{bmatrix}, \quad \mathbf{g}(k|t_j) = \begin{bmatrix} -s_1(k|t_j) + \bar{h}_{st} \\ s_1(k|t_j) - \underline{h}_{st} \\ 0 \\ v_{\max} \end{bmatrix}. \end{aligned} \quad (23)$$

We remark that  $u_d u_b = 0$  in (18) can be omitted due to the following theorem.

*Theorem 1:* The global minimizer of (22,23)  $\{\mathbf{x}(k+1|t_j), \mathbf{u}(k|t_j)\}_{k=0}^{N-1}$  yields  $u_d(k|t_j)u_b(k|t_j) = 0$ , for all  $k = 0, \dots, N-1$ .

The proof can be found in Appendix A.

The objective function in (22) is of quadratic form, while all the constraints are linear. As a result, the optimization problem (22,23) can be formulated as quadratic programming problem and can be efficiently solved. At each  $t_j$  and the first step of the solution will be applied over the interval  $[t_j, t_j + \Delta T)$  using a zero-order hold, that is,

$$u(t) = u_d(0|t_j) + u_b(0|t_j), \quad t \in [t_j, t_j + \Delta T). \quad (24)$$

Note that when implementing this on the original system (4) we enforce the original constraint (7) for  $v > v^*$ . That is we actually apply

$$u_{\min} \leq u \leq \min \left\{ u_{\max}^*, \frac{P_{\max}}{m_{\text{eff}} v} \right\}, \quad (25)$$

instead of (21); see Fig. 1(a).

#### IV. COMPARISON OF DIFFERENT CCC STRATEGIES

In this section, we compare the performance of the two frameworks through a case study of 2 + 1 vehicles. The preceding vehicles' speed profiles are shown in Fig. 3. The head vehicle's velocity  $v_2$  is generated by a PI controller with gains  $K_p = 1[1/s]$ ,  $K_i = 0.05[1/s^2]$  to follow the reference signal (red dashed curve). The next vehicle's velocity is generated by (9,10,11) using gains  $\alpha_{h,1} = 0.2[1/s]$ ,  $\beta_{h,1} = 0.3[1/s]$  that correspond to a typical human driver [18].

##### A. Feedback-based CCC

In order to optimize the fuel economy of the CCC vehicle we consider different  $\alpha$ ,  $\beta_1$ ,  $\beta_2$  combinations within  $[0, 2][1/s]$  and evaluate the fuel consumption of the HDV using numerical simulations. In Fig. 4(a), the fuel consumption is shown as surface above the  $(\alpha, \beta_1)$ -plane, so that for each  $(\alpha, \beta_1)$  pair the value is associated with the  $\beta_2 \in$

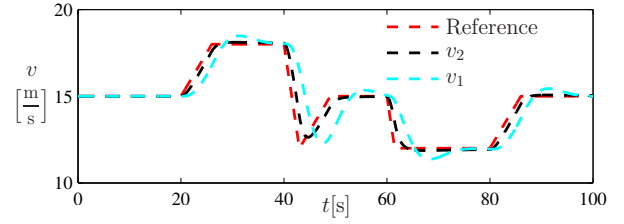


Fig. 3: Speed profile the two preceding vehicles in a (2+1)-vehicle scenario.

$[0, 2][1/s]$  that gives the least fuel consumption. To make a fair comparison with RHOC-based CCC, the constraint (25) is used and for  $v^* = 15[m/s]$  we have  $u_{\max}^* = 0.6760[m/s^2]$ . Note that the surface is only showed for those parameter combination where no collision occurs. For example, in the non-reactive case of  $\alpha = \beta_1 = \beta_2 = 0$ , collisions occur. It can be seen that for a large range of  $(\alpha, \beta_1)$ , adding  $\beta_2$  may improve fuel economy significantly.

To show how to select  $\beta_2$ , we fix  $\alpha = 0.2[1/s]$ ,  $\beta_1 = 0.3[1/s]$  and vary  $\beta_2$  between 0 and 6. The results are shown in Fig. 4(b) while the time profiles of the states  $v$ ,  $h$  and the input  $u$  are displayed in Fig. 5 corresponding to the crosses. The maximum improvement is for  $\beta_2 = 1.1[1/s]$ , which leads to 19.4% improvement compared to the case  $\beta_2 = 0$ .

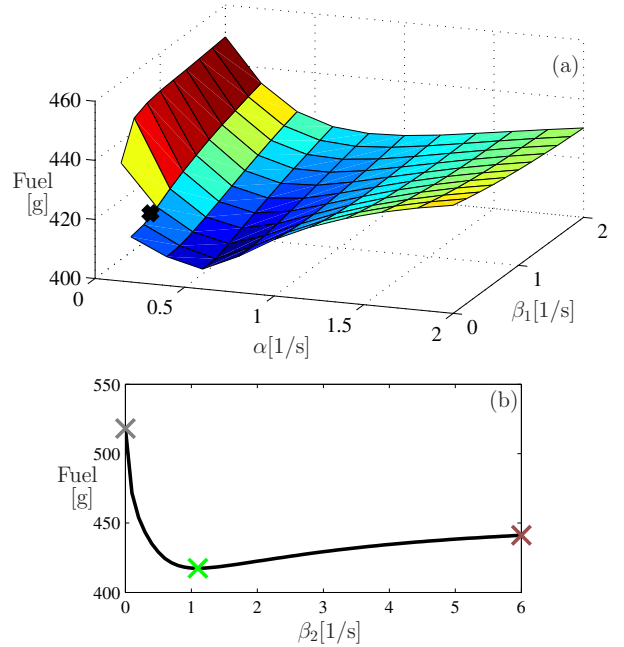


Fig. 4: (a) Fuel consumption as a function of  $(\alpha, \beta_1)$  showing the best performance within the  $\beta_2$  range  $[0, 2][1/s]$ . The black cross denotes the point associated with  $\alpha = 0.2[1/s]$ ,  $\beta_1 = 0.3[1/s]$ . (b) Fuel consumption as a function of  $\beta_2$  for  $\alpha = 0.2[1/s]$ ,  $\beta_1 = 0.3[1/s]$ . The trajectories corresponding to the crosses are displayed in Fig. 5

##### B. RHOC-based CCC

To balance accuracy and real time calculation efficiency, we set  $\Delta T = 0.1[s]$ . Moreover, we choose  $\underline{T} = 0.8[s]$ ,

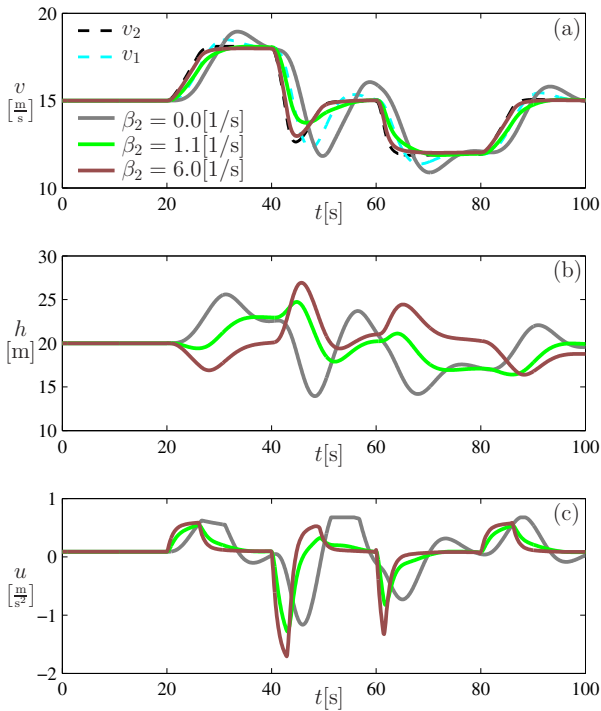


Fig. 5: Time profiles for  $\alpha_{h,1} = 0.2$  [1/s],  $\beta_{h,1} = 0.3$  [1/s],  $\alpha = 0.2$  [1/s],  $\beta_1 = 0.3$  [1/s], and different  $\beta_2$  as indicated.

$\bar{h}_{st} = 2$  [m] for the aggressive limit and  $\bar{T} = 1.2$  [s],  $\bar{h}_{st} = 8$  [m] for the cautious limit. Finally we select,  $\Delta\bar{u} = 0.4$  [m/s<sup>3</sup>],  $\Delta\bar{u} = -2$  [m/s<sup>3</sup>].

In the ideal case, the preview information about the position of the vehicle immediately ahead is accurate for long time. We are interested in is how large the benefit could be compared to the feedback controller, and how much would the improvement decrease when using inaccurate information about the motion of the preceding vehicle. For the inaccurate preview case, we assume only the current speed and acceleration of the preceding vehicle is available and construct the prediction

$$s_1(k|t_j) = s_1(t_j) + v_1(t_j)k\Delta T + \frac{1}{2}a_1(t_j)(k\Delta T)^2, \quad (26)$$

that is used in (23). Moreover, in case this prediction violates the constraint (8) the values of the velocity of the preceding vehicle are saturated at the appropriate boundary.

In Fig. 6 we compare the RHOC-based CCC using accurate as well as inaccurate information to the feedback-based CCC for the preview horizon  $T = 10$  [s]. The time evolution of  $v, h$  and  $u$  are shown in panels (a,b,c) and trajectories in the  $(h, v)$  plane are displayed in panel (d). The fuel consumptions calculated using (6) are 333.52 [g] (accurate preview), 489.84 [g] (inaccurate preview), and 417.39 [g] (feedback), respectively. By making full use of the headway limit, with accurate information, the RHOC-based CCC can achieve better performance compared to feedback controller. However, such improvement is compromised when the information is inaccurate and the fuel efficiency is even worse than that using feedback-based CCC. This example shows

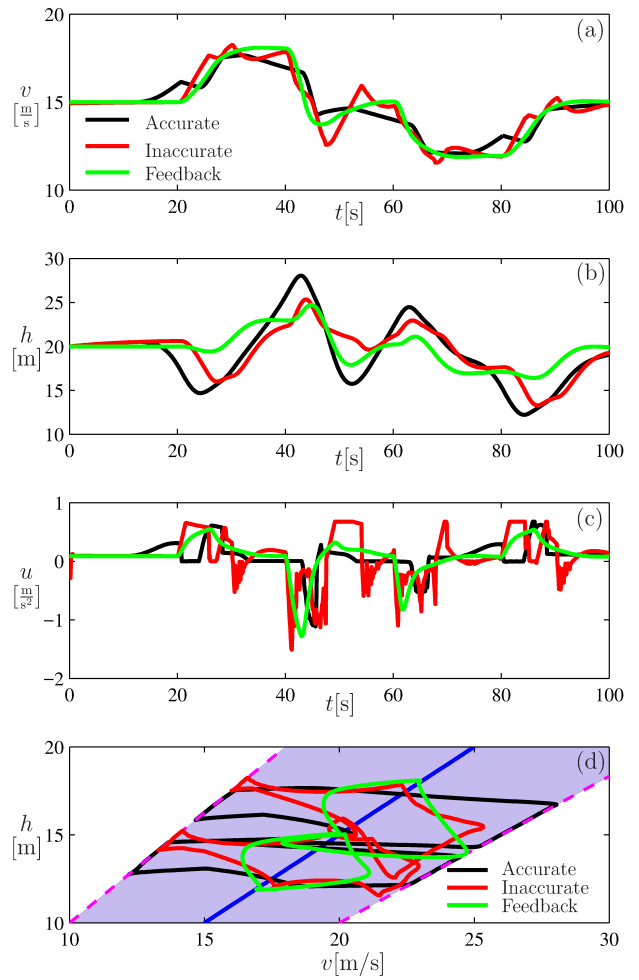


Fig. 6: (a,b,c) Time profiles for the RHOC-based CCC for preview horizon  $T = 10$  [s] with accurate or inaccurate preview information, compared with those of the feedback-based CCC for  $\alpha = 0.2$  [1/s],  $\beta_1 = 0.3$  [1/s], and  $\beta_2 = 1.1$  [1/s]. (d) The corresponding trajectories in the  $(h, v)$ -plane.

the potential large variations in fuel consumptions in RHOC-based CCC given different preview information.

To study the effect of the preview horizon, we vary  $T$  from 2 [s] to 20 [s] and summarize the results in Fig. 7. The improvements are measured compared to the  $\beta_2 = 0$  case. Even with accurate information, the RHOC-based CCC requires preview information with long enough preview horizon in order to outperform feedback-based CCC in fuel consumption. In other words the RHOC-based CCC with time horizon  $T < 5$  [s] improve the fuel economy less than the feedback-based CCC. Having longer preview horizon may improve fuel economy significantly, given accurate preview information. However, when the preview information is inaccurate, the performance is worse than the feedback-based CCC. Therefore, having a computationally expensive RHOC design may not be superior to a simple feedback-based CCC design. Furthermore, the RHOC-based CCC in general leads to larger variation in headway which may also compromise driver comfort and string stability.

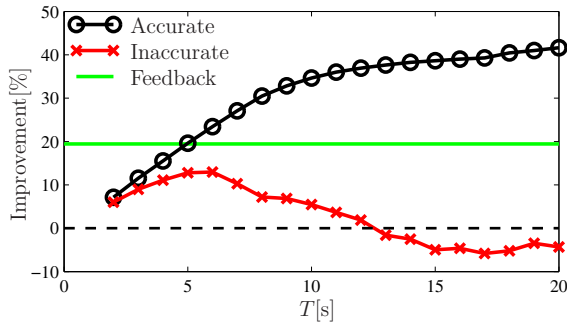


Fig. 7: Improvements of RHOC-based CCC for different values of the preview horizon  $T$ . The black circles correspond to having accurate preview information, while red crosses correspond to having inaccurate preview information. The green horizontal line corresponds to the improvement associated with the feedback-based CCC with  $\alpha = 0.2[1/s]$ ,  $\beta_1 = 0.3[1/s]$ , and  $\beta_2 = 1.1[1/s]$ . The improvements are measured for the  $\beta_2 = 0$  case.

## V. DISCUSSION AND FUTURE RESEARCH

In this paper, we compared the fuel economy of two different connected cruise control strategies exploiting information of multiple vehicles ahead acquired through vehicle-to-vehicle (V2V) communication. One was based on direct feedback structure, the other was based on optimization. We showed that feedback structure is simple, and can improve fuel economy by using instantaneous information. The optimization-based method assigned the control action in a receding horizon fashion and it requires preview information about the vehicle immediately ahead. While the optimization-based method may provide more significant fuel savings given accurate information with long enough preview time horizon, its performance was compromised significantly as the accuracy level of preview information decreased, and it performed worse than the simple feedback-based design.

## VI. ACKNOWLEDGMENTS

The authors would like to thank the NAVISTAR company for providing the source data used in this paper.

## REFERENCES

- [1] S. C. Davis, S. W. Diegel, and R. G. Boundy, "Transportation energy data book: Edition 32," U.S. Department of Energy, Tech. Rep., 2013.
- [2] U.S. Department of Transportation, "2012 commodity flow survey united states," Tech. Rep., 2014.
- [3] A. Sciarretta, G. De Nunzio, and L. Ojeda, "Optimal ecodriving control: Energy-efficient driving of road vehicles as an optimal control problem," *IEEE Control Systems Magazine*, vol. 35, no. 5, pp. 71–90, Oct 2015.
- [4] C. R. He, H. Maurer, and G. Orosz, "Fuel consumption optimization of heavy-duty vehicles with grade, wind, and traffic information," *Journal of Computational and Nonlinear Dynamics*, vol. 11, no. 6, p. 061011, 2016.
- [5] N. Kohut, K. Hedrick, and F. Borrelli, "Integrating traffic data and model predictive control to improve fuel economy," in *12th IFAC Symposium on Control in Transportation Systems*, 2009, pp. 155–160.
- [6] A. S. Sergei and G. Orosz, "Nonlinear network modes in cyclic systems with applications to connected vehicles," *Journal of Nonlinear Science*, vol. 25, no. 4, pp. 1015–1049, 2015.
- [7] M. Wang, W. Daamen, S. P. Hoogendoorn, and B. van Arem, "Cooperative car-following control: Distributed algorithm and impact on moving jam features," *IEEE Transactions on Intelligent Transportation Systems*, vol. 17, no. 5, pp. 1459–1471, 2016.

- [8] G. Orosz, "Connected cruise control: modelling, delay effects, and nonlinear behaviour," *Vehicle System Dynamics*, vol. 54, no. 8, pp. 1147–1176, 2016.
- [9] N. I. Li, C. R. He, and G. Orosz, "Sequential parametric optimization for connected cruise control with application to fuel economy optimization," in *55rd IEEE Conference on Decision and Control*, 2016, pp. 227–232.
- [10] T. G. Molnár, W. B. Qin, T. Insperger, and G. Orosz, "Predictor design for connected cruise control subject to packet loss," in *Proceedings of the 12th IFAC Workshop on Time-Delay Systems*. IFAC, 2015, pp. 428–433.
- [11] S. E. Li, Z. Jia, K. Li, and B. Cheng, "Fast online computation of a model predictive controller and its application to fuel economy-oriented adaptive cruise control," *IEEE Transactions on Intelligent Transportation Systems*, vol. 16, no. 3, pp. 1199–1209, 2015.
- [12] J. Jing, E. Ozatay, A. Kurt, J. Micheli, P. F. Dimitre, and U. Ozguner, "Design of a fuel economy oriented vehicle longitudinal speed controller with optimal gear sequence," in *55rd IEEE Conference on Decision and Control*, 2016, pp. 1595–1601.
- [13] D. Lang, T. Stanger, and L. del Re, "Opportunities on fuel economy utilizing V2V based drive systems," *SAE Technical Paper*, no. 2013-01-0985, 2013.
- [14] C. Sun, X. Hu, S. J. Moura, and F. Sun, "Velocity predictors for predictive energy management in hybrid electric vehicles," *IEEE Transactions on Control Systems Technology*, vol. 23, no. 3, pp. 1197–1204, 2015.
- [15] K. K. McDonough, "Developments in stochastic fuel efficient cruise control and constrained control with applications to aircraft," Ph.D. dissertation, University of Michigan, 2015.
- [16] C. R. He, W. B. Qin, N. Ozay, and G. Orosz, "Optimal gear shift schedule design for autonomous vehicles: Hybrid system based analytical approach," in *IEEE Transactions on Control Systems Technology*, 2017, p. Submitted.
- [17] L. Guzzella and C. H. Onder, *Introduction to Modelling and Control of Internal Combustion Engine Systems*. Springer, 2004.
- [18] L. Zhang and G. Orosz, "Consensus and disturbance attenuation in multi-agent chains with nonlinear control and time delays (published online)," *International Journal of Robust and Nonlinear Control*, vol. 27, no. 5, pp. 781–802, 2017.

## APPENDIX

### A. Proof of Theorem 1

*Proof:* We prove this theorem by contradiction. Suppose there exists  $k$  such that  $u_d(k|t_j)u_b(k|t_j) \neq 0$ , then  $u_d(k|t_j) > 0, u_b(k|t_j) < 0$ . Then one has

$$\begin{aligned} & \frac{1}{2} \begin{bmatrix} \mathbf{x}(k|t_j) \\ \mathbf{u}(k|t_j) \end{bmatrix}^T \mathbf{Q} \begin{bmatrix} \mathbf{x}(k|t_j) \\ \mathbf{u}(k|t_j) \end{bmatrix} \\ & = p_2 u_d(k|t_j) v(k|t_j) > p_2 (u_d(k|t_j) + u_b(k|t_j)) v(k|t_j) \end{aligned}$$

Thus, the sequence obtained by replacing  $u_d(k|t_j)$  and  $u_b(k|t_j)$  with  $\hat{u}_d = u_d(k|t_j) + u_b(k|t_j)$  and  $\hat{u}_b = 0$ , respectively, yields a smaller value of the objective function while it does not violate the constraints and does not change the optimal trajectory. This contradicts the fact that  $\{\mathbf{x}(k+1|t_j), \mathbf{u}(k|t_j)\}_{k=0}^{N-1}$  is the global minimizer. ■